Macromolecules

ARTICLE

pubs.acs.org/Macromolecules

Dynamically Asymmetric Phase Separation and Morphological Structure Formation in the Epoxy/Polysulfone Blends

Yan Zhang, Weichao Shi, Fenghua Chen,* and Charles C. Han*

State Key Laboratory of Polymer Physics and Chemistry, Joint Laboratory of Polymer Science and Materials, Institute of Chemistry, Chinese Academy of Sciences, Beijing 100190, China

ABSTRACT: A thermoplastic polysulfone was used to blend with epoxy resin, and both the curing reaction and phase separation of the epoxy/polysulfone blend were investigated. Polysulfone did not alter the mechanism of curing reaction; however, it did depress the reaction rate. The details of the dynamically asymmetric phase separation, which was caused by the large differences in viscoelastic properties between epoxy and polysulfone component, were observed and studied. During the structure evolution, volume-shrinking behavior of the dynamically slow polysulfone component always existed even at fairly low (but still above the entanglement concentration) concentrations. More interestingly, when the curing temperature was higher than the glass transition temperature of polysulfone, volume shrinking with the consequence of layered structure formation was also observed as long as the viscoelastic asymmetry was maintained. These results indicated the generality of the mechanism of the dynamically asymmetric phase separation in this type of reactive system. Also, the influence of curing temperature was studied, and it was found that phase separation was promoted more than the curing reaction as the temperature was increased.

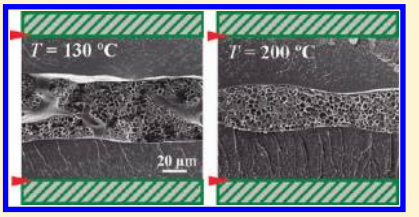

INTRODUCTION

Reaction-induced phase separation (RIPS) in epoxy/thermoplastic blend has been extensively studied due to the importance in the toughening application such as for the continuous fiber composites and also for the fundamental interest.[1−7] In an initially homogeneous epoxy/thermoplastic blend, molecular weight of epoxy increases with the curing reaction; thus, the entropy of mixing decreases. Therefore, the concentration fluctuation gradually increases, and eventually the phase separation is induced.[1,2] With different thermoplastics (TP) and curing agents used, the competition between reaction and phase separation has been qualitatively considered.[8−11] Various morphological structures, namely, sea−island, bicontinuous, or double-phase and nodular structure, have been observed in the order of increasing thermoplastic weight fraction w. Phase separation processes were followed through various measurements depending on the specific system.[12−15]

The thermoplastic polymer, e.g. poly(ether sulfone) and poly(ether imide), which was normally used to blend with epoxy, usually has a high glass transition temperature (T_g) and large molecular weight, while the epoxy component, first monomers and then oligomers because of the stepwise reaction, has low molecular weight and low T_g at the beginning. Once phase separation occurs, the TP-concentrated phase rapidly changes its behavior from solution-like to elastomer-like as the reaction, and phase separation proceeds. Dynamic asymmetry, caused by the great differences in viscoelastic behaviors between epoxy and TP due to both molecular weight and T_g, cannot be neglected in the discussion of phase-separation mechanism and has attracted some attention recently.[16−20] The dynamic asymmetry in general induces a coupling between diffusion and stress in the phase separation process. As the slow dynamic component has a long relaxation time, it cannot catch up with the deformation of the phase separation; consequently, an asymmetric stress field is induced, and unique coarsening behavior and volume shrinking of the slow dynamic component proceed as a consequence.[21−24] A three-layered structure thus formed has been reported in the previous work, where mobility of the components was compared and a speculation of the layered structure formation and phase separation kinetics was proposed.[6,19,20] In this study, more detailed and systematic experimental results on the kinetics at various thermoplastic concentrations and curing temperatures will be presented. Theory of viscoelastic phase separation is used to explain such a phase separation process, and the dynamic asymmetry between the components and the influence on phase separation mechanism will be discussed. We believe this asymmetry actually happens in many existing and well-studied systems. Therefore, a careful examination and re-examination in the cross section normal to the film specimen surface (or parallel to the surface normal) is necessary to reveal this hidden and commonly neglected but an extremely important phenomenon in order to have a correct understanding of a reaction-phase separation system like toughened epoxy blend commonly used in the continuous fiber composites.

EXPERIMENTAL SECTION

The epoxy resin used was a low molar mass liquid diglycidyl ether of bisphenol A (DGEBA), supplied by Shell Chemical Co. (product No. Epon 828). The curing agent used was 4,4′-diaminodiphenyl sulfone (DDS), purchased from Sigma-Aldrich Chem. Co. The thermoplastic component was polysulfone (PSF) (Udel P1700, M_n = 38 000),

Received: June 11, 2011
Revised: August 18, 2011
Published: September 06, 2011

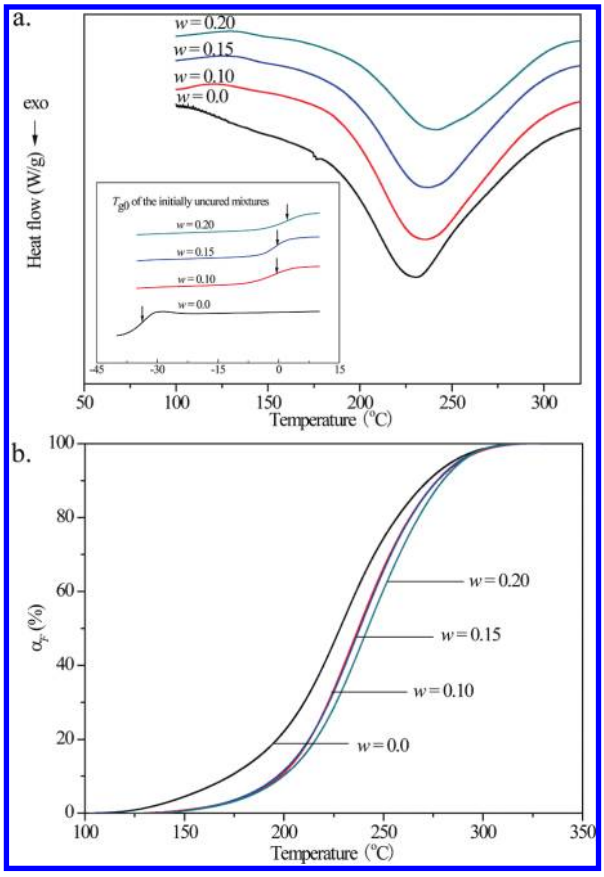

Figure 1. (a) DSC thermograms of epoxy/PSF samples with various PSF weight fractions at the scanning rate of 10 °C/min. Glass transition temperature (T_{g0}) of the initially uncured mixtures was indicated by arrows in the inset panel. (b) Fractional conversions (α_F) as a function of temperature for samples with different PSF contents.

provided by Solvay Co. Glass transition temperature of PSF, $T_{g,PSF}$, was about 183 °C, measured with a differential scanning calorimeter (Diamond DSC, Perkin-Elmer Co.). The three components were dissolved in a mixed solvent of methylene chloride and methanol. In order to adequately mix them, the solution was mechanically stirred for about 24 h. After the solvent was fully degassed, homogeneous mixtures with different initial PSF contents were obtained. The ratio of DGEBA/DDS was fixed at 1:0.27 w/w, i.e., 0.8 hydrogens of amino groups per epoxy group.

The thermograms of the curing processes were performed using a TA Q2000 differential scanning calorimeter (DSC). Nitrogen with a flow rate of 20 mL/min was used as the purge gas, and samples of 5−10 mg were used for the measurements. DSC measurements, carried out from −40 to 350 °C at scanning rate of 10 °C/min, were first performed on the initially uncured samples. Fractional conversion (α_F) at different temperatures was obtained form the equation $\alpha_F = H_T/H_0$, where H_T is the integrated area of the exotherm curve at temperature T and H_0 is the total area of the exotherm, as shown in Figure 1. The conversion (α_t) for the sample isothermally cured was obtained in the following procedure: the samples cured at a certain temperature for various intervals (corresponding to different reaction degrees) were rapidly cooled and then scanned in the DSC measurement (from −40 to 350 °C); residual heat H_r was thus obtained. α_t was calculated according to $\alpha_t = (H_0 - H_r)/H_0$, as shown in Figure 5.

Phase separation process was detected by a homemade time-resolved light scattering (TRLS) instrument. The incident beam with a wavelength of 532 nm, and a vertically polarized light was applied to the sample film. Light scattering profile was recorded every 10 s during the curing process. The sample films for TRLS, phase contrast optical microscope (PCOM), and electron microscope observation were sandwiched between two glass slides, with a poly(tetrafluoroethylene) spacer to fix the thickness during the whole curing process. After being cured for different times, the samples were immediately dipped into the liquid nitrogen so that the morphological structures were frozen for further studies. The microtomed films, 100 nm thick, were observed with a transmission electron microscope (TEM) (JEOLJEM-2200FS). The fractured and etched (by CH_2Cl_2, the solvent of PSF) surfaces were coated with platinum and then observed by a scanning electron microscope (SEM) (JEOL JSM 6700F). Samples cured for different intervals were separately prepared from the same mixture of one composition and repeated for at least three times to check the generality of the structures. Thus, morphology evolution information can be obtained.

Table 1. Characteristics of DSC Thermograms of Epoxy/PSF Samples with Various PSF Weight Fractions (w)

w	T_{g0} (°C)	T_{peak} (°C)	ΔH^a (J/g)
0	−33.5	230.1	329.0
0.10	−0.6	235.2	309.4
0.15	−0.5	236.8	285.5
0.20	1.9	241.4	225.6

[a] The reaction heat ΔH was normalized by epoxy/DDS content.

RESULTS AND DISCUSSION

The initially homogeneous samples were measured by DSC method to study the influence of PSF on the curing reaction of epoxy and DDS. As shown in Figure 1a, all the DSC curves produced broad exothermic peaks and shapes of the curves were all similar. Since the PSF is quite stable at our experimental conditions, and no functional groups can attend the reaction, the reaction mechanism of epoxy and DDS should not be changed.[25] However, with PSF content increasing, the peak temperature (T_{peak}) increased and the exothermic enthalpy (ΔH) decreased, which is shown in Table 1. The corresponding fractional conversion versus temperature of various blends is shown in Figure 1b. It showed that all the conversion values increased very slowly at low temperatures. When the samples were heated to a higher temperature (about 180 °C), the conversion values increased quickly and leveled off at temperatures higher than 300 °C. At a certain temperature, e.g. 250 °C, conversion value decreased as PSF fraction was increased, which implied that PSF depressed the epoxy curing reaction.

Because of the stepwise polymerization of epoxy and amine, molecular weight of epoxy gradually increased as the curing reaction progressed and could not be very high before gelation occurred. During this period, the reaction was controlled by the reaction kinetics but not by the monomer diffusion process.[26] As the molecular weight of the epoxy was increasing, phase separation could also start to happen. Each phase could become more and more concentrated with respect to its own component as the phase separation continued. Because of the high T_g, the PSF-rich domain should become close to its glassy state and should have a much slower or longer dynamic relaxation in both diffusion process and stress relaxation. Although the low molecular weight and low T_g ensured a good fluidity of epoxy at this early stage of reaction, the PSF molecules decreased the concentration of epoxy and DDS and thus decreased the transport rate of the

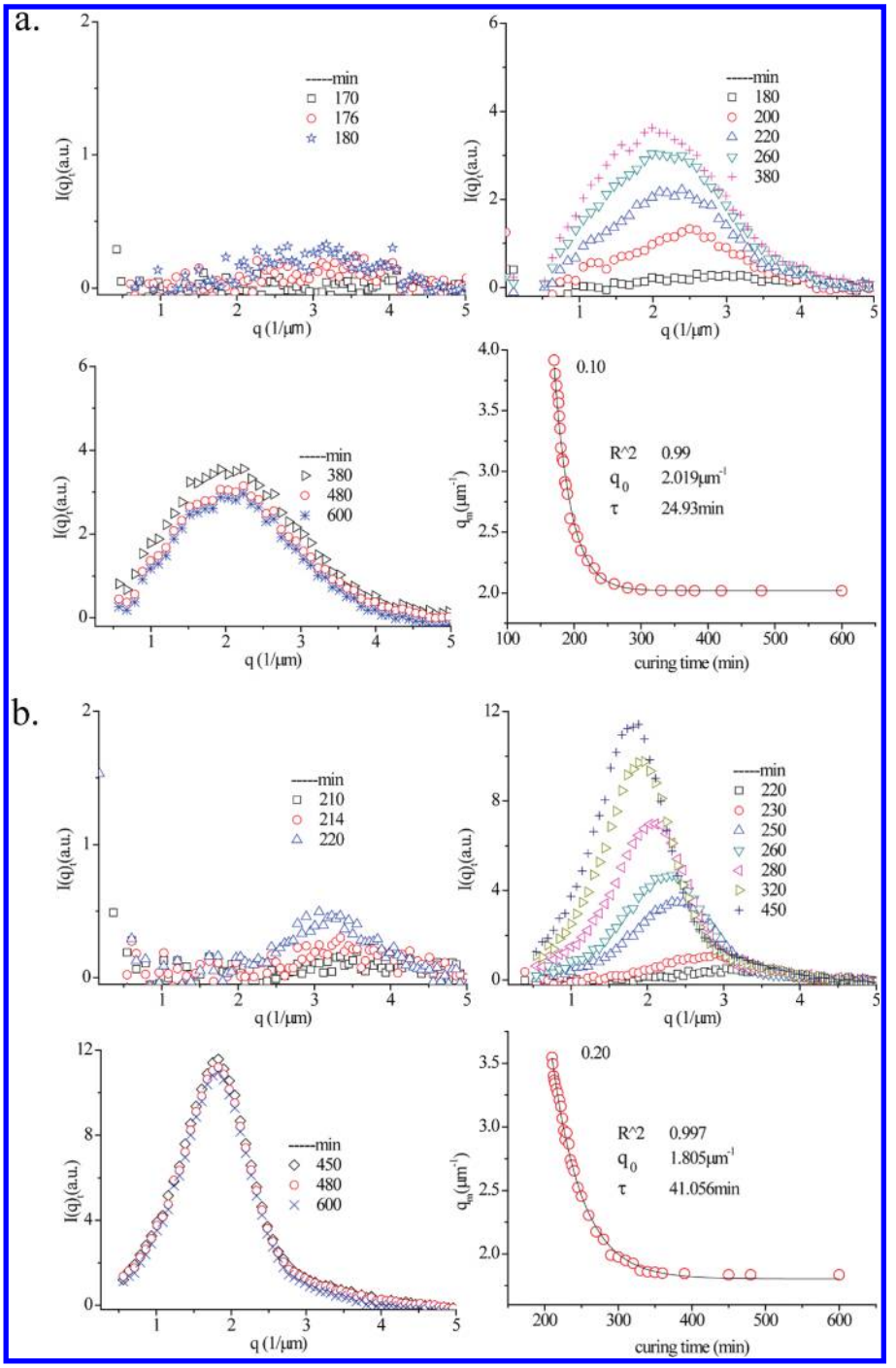

Figure 2. Variation of light scattering profiles and the corresponding q_m vs time plots for the samples w = 0.10 (a) and 0.20 (b) cured at 130 °C (a.u.: arbitrary unit for scattering intensity). In the q_m vs t, the circled points and the real line correspond to the experimental data and the result simulated by $q_m = q_0 + A_0 \exp[-(t - t_0)/\tau]$, respectively.

epoxy molecules and possibly the chemical reaction rate. With PSF content increasing, viscosity of the whole system was increased, and the actual reaction rate decreased more. A similar observation was also obtained by other authors, and physical reasons such as dilution effect and/or viscosity increase were mainly considered.[27−30] Dilution was a static average effect, while the viscoelasticity affected dynamic transport. In this system, these two effects showed the same tendency of depressing the chemical reaction.

The slow dynamics of PSF became very important during the phase separation process, and the behavior of dynamically asymmetric phase separation was observed. At certain PSF content, bicontinuous structure was formed. Then during the phase separation process, as the epoxy-rich phase showed fast growth and coarsening, the growth of continuous PSF-rich network cannot catch up and a stress field was generated by the network.[21,31] Thus, the PSF-rich network tended to shrink, and the low-viscosity epoxy-rich component tended to be

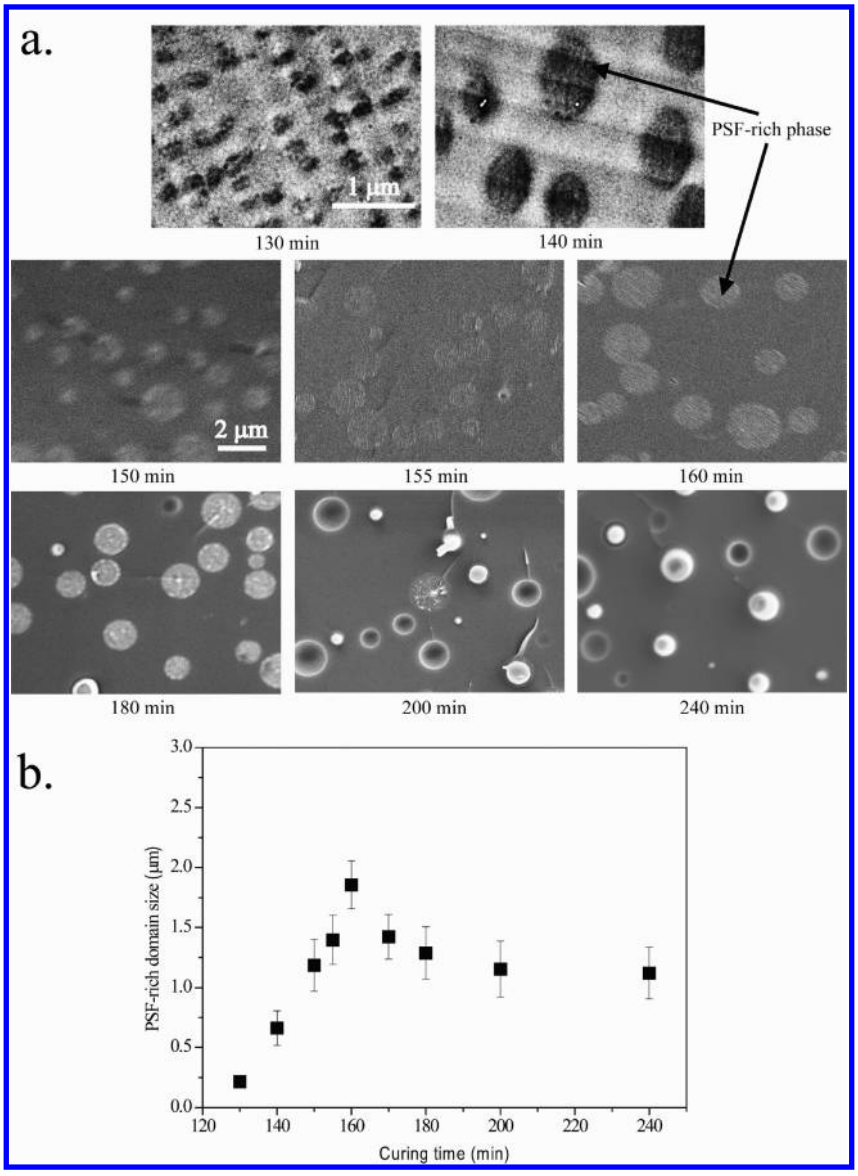

Figure 3. (a) TEM (two pictures in the first row) and SEM micrographs of the fractured surfaces of the sample $w = 0.10$ cured at 130 °C for different times. The samples for each panel were separately prepared. PSF-rich phase was indicated by the solid line with arrow to guide eyes. (b) Size changing of the PSF-rich domains for $w = 0.10$ cured at 130 °C for different time.

expelled and resulted to a three-layered structure formation, as the previous work reported.[6,19,20] At even lower or higher PSF contents, the slow dynamic property of PSF also played a great role in the phase separation process, which will be discussed in the following section.

Phase separation process of $w = 0.10$ and 0.20 was measured in situ by TRLS, and the observed information was presented in Figure 2. For the sample at $w = 0.10$, phase separation occurred at $t = 170$ min with the initial $q_m = 3.8\ \mu m^{-1}$, while for $w = 0.20$, it occurred at about $t = 210$ min with the initial $q_m = 3.5\ \mu m^{-1}$, where q_m is the peak scattering wavenumber at the maximum scattering intensity (I_m). Then in both cases, q_m and I_m gradually changed in a similar way: q_m moved slowly toward the smaller wavenumber, and simultaneously I_m became stronger and stronger, which showed the coarsening process of the phase separated domains. In the late period, q_m changed very slowly, while I_m began to decrease slightly, which was probably caused by the gradually decreasing of the refractive indices difference as the molecular weight of epoxy increasing.[19,32] Finally, q_m and I_m did not change any more due to gelation or vitrification of the system.

Variation of q_m at different times was summarized in one plot, q_m vs t, shown in the right lower part of Figure 2a,b. Here it should be emphasized that the conventional analysis of the behavior of q_m based on the scaling law (such as $q_m = t^{-\alpha}$)[33−36] is not applicable because of the absence of self-similarity in this asymmetric phase separation process. However, it was observed that the behavior of q_m with time fit well with a typical exponential decay function[16] $q_m = q_0 + A_0 \exp[-(t - t_0)/\tau]$, where A_0 is the magnifier, t_0 is the onset time of phase separation, and τ is the relaxation time of the phase separation. At $t = \infty$, $q_m = q_0$; q_0 corresponds to the dimension of the final structure at gelation or vitrification. Good fitting of this empirical equation to the experimental data and the inherent characteristics of the present system showed the viscoelastic effect (dynamic

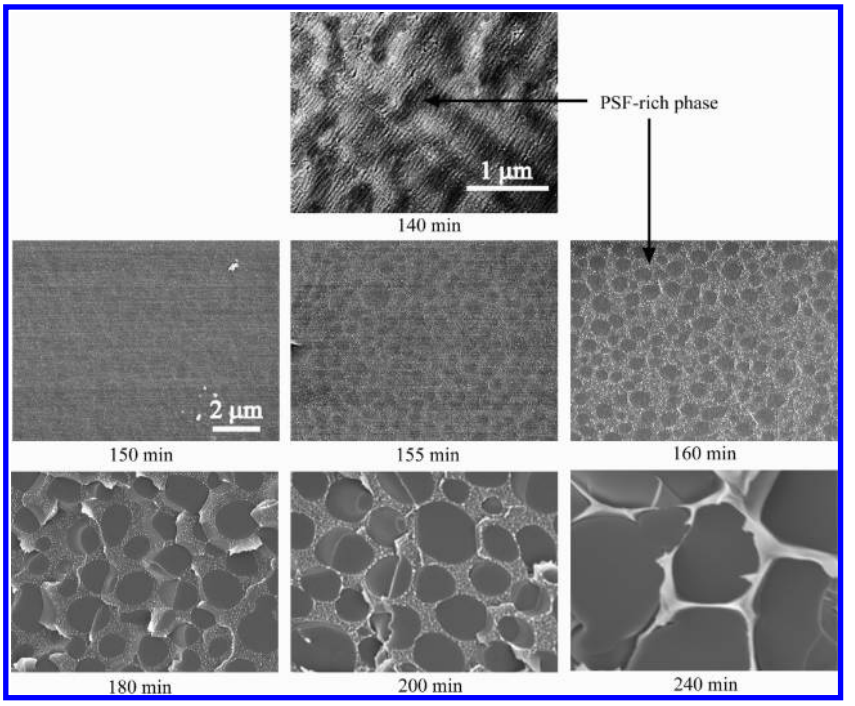

Figure 4. TEM (picture in the first row) and SEM micrographs of the fractured surfaces of sample $w = 0.20$ cured at 130 °C for different times. The samples for each panel were prepared separately. PSF-rich phase was indicated by the solid line with arrow to guide eyes.

asymmetry) dominated the phase separation process. When PSF content increased, the system would be more viscous, so the relaxation of polymer chains became slower and the relaxation time τ longer.

Further understanding of the phase separation process was shown by the electron micrographs in Figures 3 and 4, where PSF-rich phase has been indicated by the solid line with arrow. After the blend of $w = 0.10$ was held at 130 °C for $t = 130$ min, uniformly distributed PSF-rich domains could be observed as spherical particles with the average diameter of 200 nm, which must be at least close to the initial phase separation. These particles grew in size slowly. After $t = 160$ min, the PSF-rich particles would not grow but shrink instead. The volume fraction of the PSF-rich phase kept decreasing with time, and the contrast and interface between PSF- and epoxy-rich phases became more and more pronounced. The epoxy gradually transferred from the PSF-rich phase to the epoxy-rich matrix, and each phase was more and more concentrated. From $t = 200$ min on, the PSF-rich particles were rigid enough to maintain their shape during the fracture process. The particle size changed very slowly in the subsequent process. All of the data have been repeated for at least three times and could well represent the morphological structures of the whole sample. Thus, size changing information on the PSF-rich domains can be clearly observed from the statistical analysis of the SEM images, as shown in Figure 3b, where the error bar represents the root-mean-square error of that particle data point. Especially, the data at $t = 160$ min were averaged from the result of four samples with more than 1000 domains measured.

A similar but different phenomenon of volume shrinking was also observed for the sample at $w = 0.20$. Bicontinuous structure formed initially, which can be observed from the first picture shown in Figure 4. Then, the epoxy-rich phase gradually formed as droplet domains, while PSF-rich phase kept continuous. With the phase separation continuing, epoxy-rich droplets gradually grew in size, while the PSF-rich phase decreased its volume fraction and became a network. During this period, with the shrinking of the slow dynamic PSF-rich phase, the epoxy-rich phase diffused out and caused the PSF-rich network walls to become thinner and thinner. At a certain time, percolation of the epoxy-rich phase happened under the stress field of the network, and the epoxy-rich droplets can be interconnected. If the sample is quenched down in temperature, then the epoxy-rich phase showed the morphology of partially interconnected rigid particles, while the PSF-rich phase as strong and tough networks which gave a ductile fracture during the preparation of the cross-section surface sample. For even longer time, the nodular structure, interconnected irregular epoxy-rich globules, will form and morphology of the whole specimen will be fixed.

With various amounts of PSF added, dynamic asymmetry was always observed to dominate the phase separation process. This mechanism was characterized by the volume fraction change of the PSF-rich phase and was realized by the volume shrinking process of the PSF-rich domains. After phase separation was observed, it developed in the normal (symmetric system) way first, although the time period could be very short. With phase separation proceeding, PSF concentration increased, and thus its viscoelasticity also increased in the PSF-rich domains. Viscoelastic asymmetry began to control the phase separation dynamics, and accordingly the growth of normal composition fluctuation was suppressed. Instead of continuously growing in size, the slow dynamic PSF-rich domains began to shrink, and the fast dynamic epoxy-rich phase gradually diffused out. Volume shrinking of the PSF-rich domain continued until the phase separation was pinned. Finally, due to the gelation or vitrification of the system, the sea−island and nodular structures were obtained in the absence of the hydrodynamic flow regime as the usual viscoelastic phase separation.

The experiments were also carried out at different temperatures. The conversion (α_t) with respect to time (shown in Figure 5) can clearly illustrate the reaction kinetics. It showed that curing reactions at 180 and 200 °C were much faster than that at 130 °C. As expected, both phase separation and reaction must be affected by the curing temperature. The higher the curing temperature was, the faster the epoxy molecular weight increased and mixing entropy decreased, and the less time for the occurrence of phase separation was available. When the sample was cured at T_{cure} = 130 °C, phase separation was observed by PCOM at t_{ps} = 170 min, while at T_{cure} = 180 and 200 °C, t_{ps} = 20 and 12 min, respectively. When curing temperature increased, both reaction and phase separation processes were accelerated. However, as the SEM results shown in Figure 6 and Table 2, it was found that phase separation was changed more than the curing reaction.

At lower PSF concentration, w = 0.10, PSF-rich spherical domains were dispersed in epoxy matrix at all the curing temperatures. It is observed that size of the dispersed particles decreased when the curing temperature was elevated. At higher PSF contents, w = 0.20, epoxy-rich nodular structure always formed at various curing temperatures. Epoxy-rich connected particles were larger, and PSF-rich network (in between the nodules) was thinner at higher curing temperatures. In the middle PSF concentration range, w = 0.15, three-layered structure formed at all curing temperatures. Most of PSF-rich domains were located continuously in the middle layer. When the curing temperature was lower than the T_g of PSF, at T_{cure} = 130 °C, three-layered structure was extended in the whole sample film. In the middle layer, sparsely dispersed epoxy-rich particles were removed by etching but a few continuous epoxy-rich domains still existed. However, when the curing temperature was close to or higher than T_g of PSF, i.e. $T_{cure} \geq$ 180 °C, the three-layered structure was somewhat disconnected, where sea−island structure formed instead, and the layered and sea−island structures coexisted in the whole sample film. For the layered structure, connected epoxy-rich particles (similar to the nodular structure formed at higher PSF contents) formed in the middle layer. The higher the curing temperature was, the more disconnections occurred in the layered structure and the smaller the size of the connected epoxy-rich particles in the middle layer was.

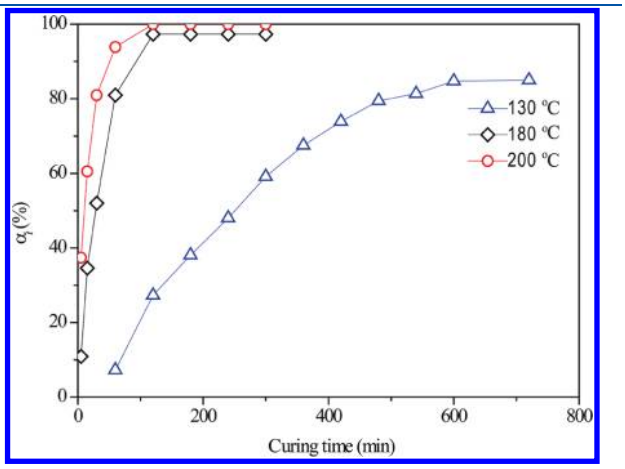

Figure 5. Conversion (α_t) vs time curves for w = 0.15 cured at various curing temperatures for different times. The open symbols are related to the experimental data points, and solid lines are only to guide the eyes.

Table 2. Periodical Distance of Final Structures (a), Measured by TRLS for w = 0.10 and 0.20 and the Relative Thickness of Middle Layer (b), Statistically Summarized from the SEM Results for w = 0.15

	samples		
T_{cure} (°C)	w = 0.10[a] (μm) (periodic distance)	w = 0.15[b] (%) (middle layer thickness)	w = 0.20[a] (μm) (periodic distance)
130	2.5	40	5.9
160	2.7	34	11.8
180	2.9	29	13.1
200	3.0	28	13.7

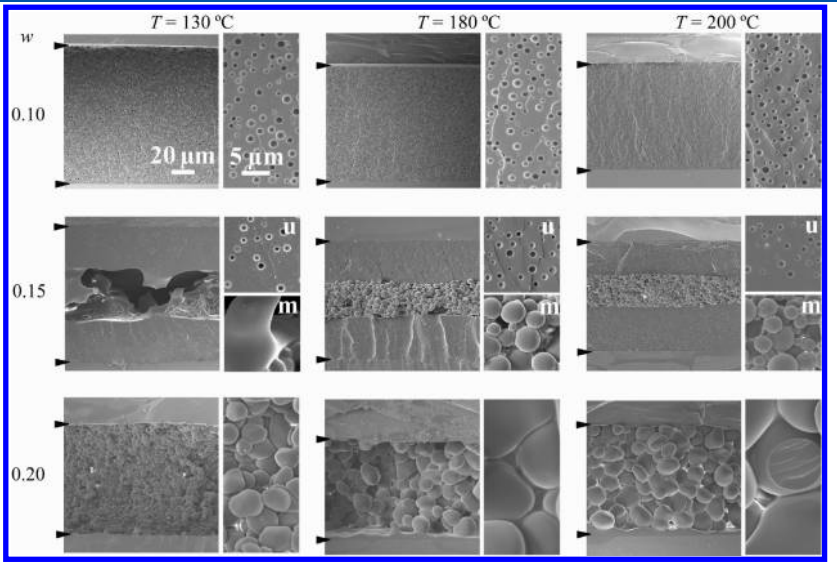

Figure 6. SEM micrographs of fractured surfaces of epoxy/PSF mixtures with different amounts of PSF cured at various temperatures for 1440 min. Right side pictures in each panel are at the higher magnifications. For w = 0.15, the upper (u) and middle (m) parts are shown. Voids correspond to the PSF-rich domains.

dx.doi.org/10.1021/ma201318g |*Macromolecules* 2011, 44, 7465–7472

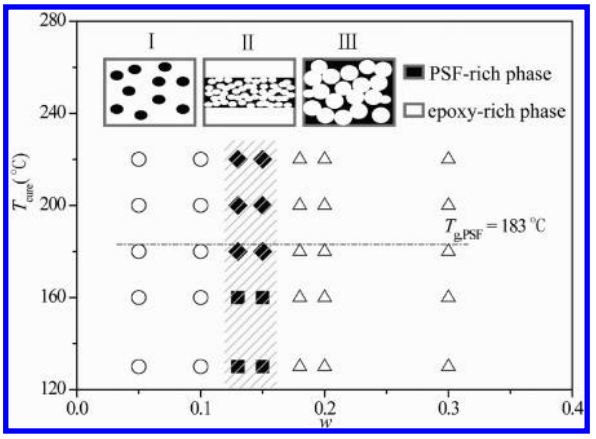

Figure 7. Curing temperatures (T_{cure}) and PSF weigh fractions (w), at which various morphological structures were observed: I, sea−island structure (○); II, three-layered structure (■), three-layered coexisted with sea−island structure (◆); III, nodular structure (△). The dashed line, corresponding to the $T_{g,PSF}$, was only to guide the eyes. The shadowed area showed where three layers could be observed. Model morphology was mapped correspondingly in the top of the figure.

In the same composition range, similar morphological structures always formed at any of the curing temperatures, no matter which were lower or higher than the $T_{g,PSF}$. The composition ranges, lower, middle, and higher, are summarized in Figure 7, and the corresponding morphologies are attached as I, II, and III, respectively. That is to say: I, sea−island structure; II, three-layered structure; and III, nodular structure. It suggested that PSF-rich phase always behaved as a slow dynamic component at the various temperatures. When the curing temperature was increased, the mobility of PSF was enhanced, which made the disentanglement of the PSF chains easier and thus the epoxy can separate from PSF-rich phase more easily. Therefore, periodical distance of final structures for both w = 0.10 and 0.20 increased while the relative thickness of middle layer for w = 0.15 decreased at increasing temperatures. And more complicate layered structure formed at higher temperatures for w = 0.15, since some parts of the PSF-rich network could be broken and most of the large continuous epoxy-rich phase could flow out under the stress field of the deformed PSF-rich network.

The influence of PSF on phase separation can be understood by the schematic phase diagram shown in Figure 8. First, in order to confirm the upper critical solution temperature (UCST) type of phase diagram for this reactive system, we designed a simple experiment as follows. The initially homogeneous sample was held at 130 °C for a given time. When phase separation was just about to occur, the sample was rapidly quenched to 100 °C. Phase structures could be clearly observed immediately. It indicated that the UCST-type phase behavior existed in this system.

Second, the initial coexistence curve was quite asymmetrical due to the molecular weight difference of the two components, with the critical concentration located at a low PSF concentration (the phase diagram skewed to the epoxy side). With the curing reaction continuing, the molecular weight of epoxy kept increasing, the phase diagram gradually moved upward, and critical temperature and composition also increased. According to the lever rule in the phase diagram, volume fraction of the PSF-rich phase should continuously decrease after the initial growth. During the phase separation process, the volume shrinking phenomenon of the PSF-rich domains was observed (Figure 8a).

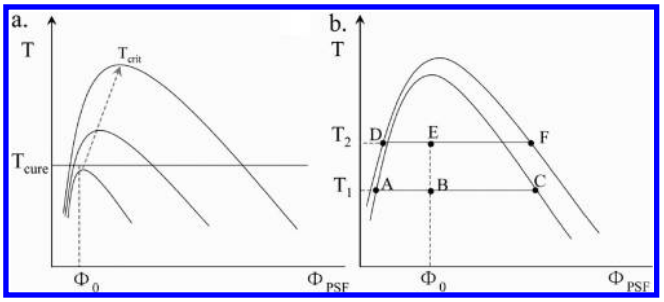

Figure 8. Schematic phase diagram of DGEBA/DDS/PSF during curing reaction (a) and phase diagrams at gel point of the system (b).

Third, in this reactive system, phase separation was slowed down and prevented by the epoxy gelation. Although reaction continued some more after gel point, the phase morphology was almost pinned and phase separation can only proceed in the very local region; i.e., phase separation was almost stopped by gelation.[37] This could also be understood from the viewpoint that reaction only proceeded in the quite localized region after gelation. Thus, we can assume that the phase diagram at gel point is the final one.

As the molecular weight of epoxy can not be very high until the gel point, the asymmetric phase diagram could be effectively used in the discussion of the final morphologies. Although theoretical gelation takes place at a defined conversion, most experimental values were higher than theoretical and showed a trend of increase of conversion with the increase of curing temperature.[28,38,39] A perfectly growing network (a random distribution of reaction sites in the uniformly distributed epoxy monomers and cross-linkers) in the theoretical gelation calculation may be different from the real case, where hanging chains and intramolecular reactions usually take place.[39] At high temperatures, reaction and side reaction rates are much faster than that at low temperatures; however, the competition between reaction and diffusion may promote more local than global reaction, which is needed to extend the cross-linked structure to the whole sample and reach the gel point. Therefore, the asymmetric phase diagram at gel point for the sample cured at T_2 need higher conversion and consequently will shift toward higher temperature than that at T_1, here $T_2 > T_1$. After phase separation developed and being pinned at the gelation point, the initial concentration Φ_0 would phase separated into the corresponding coexistence compositions of A, C at T_1, and D, F at T_2. Since DE/EF < AB/BC, total volume fraction of the PSF-rich phase at T_2 was less than that at T_1; i.e., phase separation proceeded more with the increase of curing temperature (Figure 8b). Therefore, periodical distance of the final structures increased with temperature at lower and higher PSF contents, and thinner middle layer was observed at higher temperatures in the middle PSF contents.

When the reaction and phase separation took place at temperatures lower than $T_{g,PSF}$, the PSF-rich phase behaved approximately like a glass when it was concentrated enough. At temperatures higher than $T_{g,PSF}$, the PSF-rich phase behaved as viscous elastomers. It indicated that the PSF-rich phase always showed slower dynamical behaviors compared with the fast dynamics of epoxy-rich phase. Therefore, the influence of dynamic asymmetry on phase separation and final morphologies was always significant, and the overall structures formed at any w were qualitatively similar and did not drastically change at different curing temperatures. However, for very low concentration (like w = 0.10) before a tight entanglement network can be formed, the asymmetric phase separation

behavior was less obvious. Also, at any even higher temperatures, the more extended curing reaction will make all behaviors similar to that of decreasing concentration of PSF.

CONCLUSION

We investigated the reaction-induced phase separation of epoxy/DDS/PSF blend in this work. It was found that reaction of epoxy and DDS was depressed by the PSF, while qualitatively the reaction mechanism did not change. Because of the high glass transition temperature and high molecular weight, PSF behaved as a slow dynamic component during the phase separation process. More interestingly, the asymmetric properties between the components always dominated the phase separation process even at fairly low (but still above the entanglement concentration) concentrations and temperatures lower or higher than the T_g of PSF. Volume shrinking of the PSF-rich domains was observed for all of the samples cured at various temperatures, which illustrated the action of dynamically asymmetric phase separation mechanism. When the temperature was increased, both reaction and phase separation rate were accelerated, while phase separation was changed more. The enhancement of PSF dynamics at higher temperatures made it easier for epoxy to separate from the PSF-rich phase. Thus, larger periodic length was observed for the structures formed at lower and higher PSF concentrations, and thinner relative thickness was obtained for the layered structure formed at middle PSF contents. Qualitatively, with the increase of temperature (for PSF concentration higher than its entanglement concentration), the system behaved similar to that at lower concentrations.

AUTHOR INFORMATION

Corresponding Author

*Ph +86 10 82618089; Fax +86 10 62521519; e-mail fhchen@iccas.ac.cn (F. Chen), c.c.han@iccas.ac.cn (C.C. Han).

ACKNOWLEDGMENT

This work is supported by National Natural Science Foundation of China, No. 20904062 and NSFC 50930003.

REFERENCES

(1) Inoue, T. *Prog. Polym. Sci.* **1995**, *20*, 119–153.
(2) Williams, R. J. J.; Rozenberg, B. A.; Pascault, J. P. *Adv. Polym. Sci.* **1997**, *128*, 95–156.
(3) Martinez, I.; Martin, M. D.; Eceiza, A.; Oyanguren, P.; Mondragon, I. *Polymer* **2000**, *41*, 1027–1035.
(4) Francis, B.; Poel, G. V.; Posada, F.; Groeninckx, G.; Lakshmana Rao, V.; Ramaswamy, R.; Thomas, S. *Polymer* **2003**, *44*, 3687–3699.
(5) Rebizant, V.; Venet, A. S.; Tournilhac, F.; Girard-Reydet, E.; Navarro, C.; Pascault, J. P.; Leibler, L. *Macromolecules* **2004**, *37*, 8017–8027.
(6) Chen, F. H.; Wang, X.; Zhao, X. J.; Liu, J. G.; Yang, S. Y.; Han, C. C. *Macromol. Rapid Commun.* **2008**, *29*, 74–79.
(7) Amendt, M. A.; Chen, L.; Hillmyer, M. A. *Macromolecules* **2010**, *43*, 3924–3934.
(8) Bonnet, A.; Pascault, J. P.; Sautereau, H.; Camberlin, Y. *Macromolecules* **1999**, *32*, 8524–8530.
(9) Bonnet, A.; Pascault, J. P.; Sautereau, H.; Taha, M.; Camberlin, Y. *Macromolecules* **1999**, *32*, 8517–8523.
(10) Swier, S.; Mele, B. V. *Macromolecules* **2003**, *36*, 4424–4435.
(11) Swier, S.; Assche, G. V.; Vuchelen, W.; Mele, B. V. *Macromolecules* **2005**, *38*, 2281–2288.
(12) Park, J. W.; Kim, S. C. *Polym. Adv. Technol.* **1996**, *7*, 209–220.
(13) Jin, J. Y.; Cui, J.; Tang, X. L.; Ding, Y. F.; Li, S. J. J.; Wang, J. C.; Zhao, Q. S.; Hua, X. Y.; Cai, X. Q. *Macromol. Chem. Phys.* **1999**, *200*, 1956–1960.
(14) Francis, B.; Rao, V. L.; Poel, G. V.; Psaada, F.; Groeninckx, G.; Ramaswamy, R.; Thomas, S. *Polymer* **2006**, *47*, 5411–5419.
(15) Kim, J. T.; Kim, H. C.; Kathi, J.; Rhee, K. Y. *J. Mater. Sci.* **2008**, *43*, 3124–3129.
(16) Gan, W. J.; Yu, Y. F.; Wang, M. H.; Tao, Q. S.; Li, S. J. *Macromolecules* **2003**, *36*, 7746–7751.
(17) Yu, Y. F.; Wang, M. H.; Gan, W. J.; Tao, Q. S.; Li, S. J. *J. Phys. Chem. B* **2004**, *108*, 6208–6215.
(18) Jose, J.; Joseph, K.; Pionteck, J.; Thomas, S. *J. Phys. Chem. B* **2008**, *112*, 14793–14803.
(19) Chen, F. H.; Sun, T. C.; Hong, S.; Meng, K.; Han, C. C. *Macromolecules* **2008**, *41*, 7469–7477.
(20) Zhang, Y.; Chen, F. H.; Shi, W. C.; Liang, Y. R.; Han, C. C. *Polymer* **2010**, *51*, 6030–6036.
(21) Tanaka, H. *Phys. Rev. Lett.* **1996**, *76*, 787–790.
(22) Tanaka, H. *J. Phys.: Condens. Matter* **2000**, *12*, 207–264.
(23) Wang, X.; Okada, M.; Matsushita, Y.; Furukawa, H.; Han, C. C. *Macromolecules* **2005**, *38*, 7127–7133.
(24) Wang, X.; Okada, M.; Han, C. C. *Macromolecules* **2006**, *39*, 5127–5132.
(25) Prolongo, M. G.; Arribas, C.; Salom, C.; Masegosa, R. M. *J. Appl. Polym. Sci.* **2007**, *103*, 1507–1516.
(26) Moroni, A.; Mijovic, J.; Pearce, E. M.; Foun, C. C. *J. Appl. Polym. Sci.* **1986**, *32*, 3761–3773.
(27) Girard-Reydet, E.; Riccardi, C. C.; Sautereau, H.; Pascault, J. P. *Macromolecules* **1995**, *28*, 7608–7611.
(28) Ishii, Y.; Ryan, A. J. *Macromolecules* **2000**, *33*, 167–176.
(29) Gonzalez-Benito, J.; Esteban, I. *Colloid Polym. Sci.* **2005**, *283*, 559–569.
(30) Blanco, M.; López, M.; Fernández, R.; Martin, L.; Riccardí, C. C.; Mondragon, I. *J. Therm. Anal. Calorim.* **2009**, *97*, 969–978.
(31) Taniguchi, T.; Onuki, A. *Phys. Rev. Lett.* **1996**, *77*, 4910–4913.
(32) Kim, B. S.; Chiba, T.; Inoue, T. *Polymer* **1995**, *36*, 67–71.
(33) Binder, K. *Phys. Rev. A* **1984**, *29*, 341–349.
(34) Hashimoto, T.; Itakura, M.; Shimidzu, N. *J. Chem. Phys.* **1986**, *85*, 6773–6786.
(35) Fratzl, P.; Lebowitz, J. L.; Penrose, O.; Amar, J. *Phys. Rev. B* **1991**, *44*, 4794–4811.
(36) Edel, V. *Macromolecules* **1995**, *28*, 6219–6228.
(37) Kim, B. S.; Chiba, T.; Inoue, T. *Polymer* **1993**, *34*, 2809–2815.
(38) Barral, L.; Cano, J.; López, J.; Nogueira, P.; Ramírez, C.; Abad, M. J. *Polym. Int.* **1997**, *42*, 301–306.
(39) López, J.; Ramírez, C.; Torres, A.; Abad, M. J.; Barral, L.; Cano, J.; Díez, F. J. *J. Appl. Polym. Sci.* **2002**, *83*, 78–85.